

# Inversion in Geology by Interactive Evolutionary Computation

Chris Wijns<sup>a,b,\*</sup>, Fabio Boschetti<sup>a</sup>, Louis Moresi<sup>a</sup>

<sup>a</sup>*CSIRO Exploration and Mining, PO Box 437, Nedlands, WA 6009, Australia*

<sup>b</sup>*Dept. Geology and Geophysics, University of Western Australia, Nedlands, WA 6907,  
Australia*

---

## Abstract

We present a first step towards the development of a system that would allow geological models to evolve backwards in time. The method of interactive evolutionary computation provides for the inclusion of geological knowledge and expertise in a rigorous mathematical inversion scheme, by simply asking an expert user to visually evaluate different geological models. The potential of the technique is demonstrated for examples of faulting and folding.

*Key words:* Inversion, interactive evolutionary computation, modelling, visualisation

*PACS:* 07.05.Mh, 07.05.Tp, 02.50.Sk

---

## 1 Introduction

In recent years fast computers have allowed the development of quite sophisticated forward modelling of geological processes. Plate tectonics, faulting and folding,

---

\* Corresponding author.

*Email address:* cwijns@geol.uwa.edu.au (Chris Wijns).

mantle convection, and fluid flows can all be treated in a rigorous numerical fashion, much in the same way as traditional geophysical applications such as seismic or potential field problems.

In general, forward modelling allows us to answer questions such as “What response should I expect under these initial conditions?” (e.g. “What faults will be generated by this stress field in this material?”, “What convection pattern will be generated by this temperature gradient?”, “With this slope will this open pit be stable?”, and so on.). The answer is obtained by providing a computer code with certain input parameters, running the code for a number of time steps, and looking at the final result, most often in the form of a geological section or 3D model.

However, most real world problems, including geological ones, require an answer to a question that goes in the opposite direction, i.e., “What initial conditions may result in this geological response?” (e.g. “What stress field can generate these faults?”, “What temperature gradient can produce this mantle convection pattern?”, or “What slope will allow this open pit to be stable?”). This is a far more complicated mathematical problem, for which an analytic solution rarely exists. More often, the answer must be found by iterative numerical trial and error methods, that are very computationally intense, often mathematically unstable, and frequently cannot provide an exact solution. In applied mathematics and engineering this goes under the term *inverse theory*, or simply *inversion* (Tarantola, 1987).

We believe that inversion is the natural step forward in geological modelling. The potential of such an application would be tremendous given that, broadly speaking, reconstructing initial geological configurations from their geological responses is very much what geology is about, and is an implicit inverse problem tackled on a daily basis by every geologist.

The reality of inversion involves difficult mathematical hurdles. To the underlying non-uniqueness and instabilities of the mathematical problem, we must add complexities prevalent in geology. This includes incomplete knowledge of the geological process itself as well as a lack of exhaustive data. Data are most often comprised of occasional outcrops (sparse 2D data) for problems that are clearly four-dimensional (volume plus time evolution).

To overcome these many difficulties, geologists use their intuition and experience to focus only on the “geologically reasonable” models which lead to the particular formations they observe. There is, of course, a danger that their experience and intuition will filter out physically valid models which they have not previously encountered. In our approach we have combined the formal methodology of mathematical inversion with the geologist’s expert knowledge, in order to unravel the mechanical evolution of a geological formation.

The power of this approach lies in the wide variety of applications with which it can deal. In this paper we present experiments in modelling extensional faulting, multiple wavelength folding, and convective thermal profiles in the mantle. The technique we propose can help every time a problem needs visual appraisal of the results or experience and a priori knowledge. All that is required is a code that allows the user to forward model a process and view its result.

## **2 Method**

At present, geological modelling is almost exclusively confined to the forward modelling stage. The quality of a solution is often judged according to its resemblance to patterns seen in the field, to the fact that it does not contradict basic geologi-

cal principles, or simply to the modeller's a priori expectations. Fit to data can be used as a further criterion when available, but this is rarely possible in a formal mathematical way.

Recently, research in artificial intelligence has resulted in systems to support artistic creativity (Takagi, 2001). They have been used, for example, in graphic design and music composition. The systems take advantage of fast computation to generate a suite of images or music sequences. An artist looks at the different images or listens to pieces of music and ranks them according to his or her preferences. An inversion strategy takes into account such judgement in a formal mathematical way to generate a new set of images or music sequences, iteratively converging towards the artist's tastes. This technique for directing the search through parameter space is called interactive evolutionary computation (IEC).

We have extended the use of such techniques to geological applications in which subjective judgment is necessary to evaluate geological models in the absence of sufficient constraints. We believe the system represents an advance on traditional, time-consuming trial and error approaches by providing a formal role for relevant geological experience and knowledge in inversion. The traditional numerical measure of data mismatch is replaced by the user's subjective evaluation. Humans find it hard to express subjective judgment with absolute values, while they generally find it much easier to compare different instances of the same process and rank them according to certain criteria. Consequently, interactive inversion works by producing different possible solutions and presenting them to the user for judgment and ranking.

Genetic algorithms (GAs) are a search method suitable for the inversion of highly non-linear functions. Starting with a set of random solutions, these algorithms pro-

gressively modify the solution set by mimicking the evolutionary behavior of biological systems (selection, cross-over and mutation), until an acceptable result is achieved. Since GAs work by optimising an ensemble of solutions, unlike other inversion algorithms that optimise one single solution, they are an obvious choice as the internal engine for interactive inversion applications.

GAs are an established technique today, with a wide range of applications to both theoretical and industrial problems. We refer the reader to Goldberg (1989) for a basic description of GAs and to Boschetti et al. (1996), for a more detailed description of the specific GA implementation used in this work. The mathematically oriented reader may also refer to Boschetti and Moresi (2001) for a discussion on the implications of subjective evaluation on the search space landscape and convergence speed.

Our IEC system works by linking a geological forward model to a GA. The forward modelling code used here is a particle-in-cell finite element code which is well suited to problems involving very large deformation. Details of this code can be found in Moresi and Solomatov (1995) as well as on the World Wide Web at <http://www.ned.dem.csiro.au/research/solidMech/PIC/Ellipsis.htm>. The inversion process works as follows: a geologist uses the computer code with the aim of producing a geological model that matches a target geological section. A number of selected parameters is allowed to vary within given ranges. The GA initially generates a suite of different models using randomly picked parameter values. In our case, these models could be static geological models or animations showing time evolution. Present scientific technology does not admit an automated method of discriminating between geologically appropriate results, so the geologist ranks each of them according to geological criteria, guided by his or her experience and knowledge. Once the results are ranked, the GA applies mathematically rigorous

methods to generate a new set of models that progressively converges towards the target geological section. An element of randomness is also part of the approach, allowing unexpected models to be generated and perhaps suggesting new possibilities outside the experience or expectation of the geologist.

### **3 Results**

#### *3.1 Faulting*

The first example seeks to reproduce common extensional structures in a rifting environment. The ranking of forward model results is based upon comparison with a target image, in this case the simplified line sketch of Fig. 1(a). Although the forward models evolve in time, in this introduction to our inversion method, only the final configurations are used for visual evaluation. The model is composed of two initially homogeneous crustal layers, on top of which is a low density, low viscosity background material which does not interfere with the mechanics of the problem. This initial configuration is illustrated in Fig. 1(b), in which the box has an aspect ratio of four. We are scaling to a true height of 15 km, which includes an upper crustal thickness of 9 km, and the top 3 km of the lower crust. The upper crust has strain-softening properties, which cause initial strain perturbations to localise. We include such an initial weakness in the upper layer in order to control the location of the first fault. This perturbation is small enough that it does not affect the direction or depth of fault propagation. The fault geometry and successive fault spacing arise naturally from the initial conditions of the problem. Strain-softening is our approximation to brittle behaviour in the upper crust – a yield law prescribes an

upper limit  $\sigma_y$  on the stress according to

$$\sigma_y = (B_o + B_p p) f(\varepsilon)$$

where  $p$  is the pressure,  $B_o$  is the cohesion, or yield stress at zero pressure, and  $B_p$  is the pressure dependence of the yield stress. Strain softening is included through the power law function  $f(\varepsilon)$ , in which  $\varepsilon$  is the accumulated plastic strain.

$$f(\varepsilon) = \begin{cases} 1 - (1 - E_a) (\varepsilon/\varepsilon_o)^2 & \varepsilon < \varepsilon_o \\ E_a & \varepsilon \geq \varepsilon_o \end{cases}$$

The coefficients  $E_a$  and  $\varepsilon_o$  are arbitrary parameters in the strain-softening law. The “saturation” strain  $\varepsilon_o$  is the point beyond which no further strain softening takes place, and at this point the maximum proportion of strain weakening is given by  $E_a$ . We also include a failure criterion in tension using a parameter  $B_c$  which represents the (isotropic) stress limit in tension. Beyond this limit we assume failure, which in our continuum case is approximated by an immediate thousandfold reduction in the yield stress  $\sigma_y$ .

Eight forward models are run at each step of the inversion. We allow six upper crustal strength parameters to vary: viscosity and the five yield law coefficients described above. These variables are also listed in Table 1.

Extension proceeds by applying a uniform velocity to the right-hand boundary. Fig. 1 illustrates the evolution of results using the IEC algorithm. We infer that bands of high localised strain represent faults. Accumulated strain is indicated by areas of darkened material, and the degree of shading is indicative of the amount of strain. The first panel (i) contains no models which resemble the target image. In fact, only two models have converged numerically and been extended to full length. Models

6 and 8 exhibit structures penetrating the upper crust, and for this reason they are ranked first and second, respectively. The other models do not merit ranking, but are nonetheless weighted randomly by the GA in order to fill up the remaining six positions.

Panel ii of Fig. 1 contains the second iteration of the algorithm. Once again there are four models which do not converge numerically, but those that do converge generally display more crustal-scale structures than in the first iteration. The rank of each model result is noted below each image. We continue iterating in this manner a total of six times, at which point half of the resulting images are qualitatively similar to the target image (Fig. 1, panel iii), and the process is halted.

The outcome of this experiment is a set of crustal strength parameters that leads to the behaviour observed and inferred in the field. These (dimensionless) parameters are listed in Table 1, together with their initial ranges, the final values which give rise to the highest-ranked model of the final generation (Fig. 1, panel iii, third model), and the range of each parameter for the four top-ranked models of the final generation. We can draw a few conclusions from these final values. Considering that we have set the lower crustal viscosity at 200, the upper crust must have a viscosity which is about 45 times as great, in order for faulting to occur instead of simple viscous stretching. This viscosity factor is in conjunction with a value of  $E_a$  which indicates a minimum  $\sigma_y$  of 20% of the original strength after maximum strain weakening, and a low limit in tension before yielding. The algorithm settles on low surface cohesion values, but the pressure dependence, when scaled according to the problem, is roughly equivalent to a yield strength increase of about 4 MPa/km. This is quite close to the gradient given by Byerlee's Law for a dry crust (Brace and Kohlstedt, 1980). Looking at the final range of the saturation strain  $\varepsilon_o$ , we note that this parameter may vary more significantly without affecting the crustal behaviour.

### 3.2 Folding

In this next problem, we would like to investigate the conditions which promote the development of multiple simultaneous folding wavelengths as a box of layered material (Fig. 2a) is compressed from one end. There is an initial wavelength present, and we look for the appearance of at least one more wavelength, in contrast to observing only the passive amplification of the initial perturbation. We do not refer to any target image, as in this example our target is deliberately vague. We in fact set out to explore the diversity of parameter combinations which are capable of producing any kind of multiple wavelength folding. We allow the GA to vary the layer viscosities and thicknesses as well as their yield stresses.

Fig. 2(b) shows the fifth and final generation of the algorithm, in which half of the outcomes display multiple wavelengths of folding. An analysis of the input parameters shows us that such behaviour depends upon the presence of at least one layer with high viscosity and yield stress (*i.e.* strong) and at least one layer which is substantially weaker, either through a low viscosity or a low yield stress. We have discovered two different mechanisms which lead to similar results. The variety of different results which is deemed acceptable is indicative of the variation in the other parameters, *i.e.* which layers are strong or weak, and relative thicknesses.

## 4 Discussion

In the above examples we wish to arrive at some particular behaviour of the crust during deformation. Finding a suitable combination of parameters which gives rise to this behaviour would previously have involved one of two more laborious approaches: the manual selection of parameters by trial and error, or an exhaustive

coverage of all parametric space. Trial and error may succeed with a limited number of parameters, but depends upon the user's knowledge of the coupling and feedback between parameters, which, in highly non-linear problems involving complex crustal rheologies, may be impossible. A parametric study quickly becomes unfeasible due to the sheer number of models which must be run as the number of parameters is increased. In the extension problem, in excess of 650 000 models would have to be run in order to cover all possible parameter combinations. Neither of these approaches takes full advantage of the expert knowledge of a field geologist, who may for example have a limited grasp of numerical modelling or physics, but a vast store of observational experience.

Our IEC method can be used by a field expert to invert for model parameters through the comparison of suitable images. The first case, involving faulting of the crust, is an example of a specific inversion target where an image has replaced a numerical target. The GA converges upon a set of parameters which allows us to reproduce the conceptual model of the geologist. In this manner, assuming that we have constrained the input parameters to be physically realistic, we are able to validate the conceptual model. The folding example illustrates the use of the IEC algorithm as a classification tool, where a ranking is arguable. The GA gradually accumulates more models in the appropriate (subjective) category. The analysis of the results in this case is more complicated and involves sifting through the history of the different generations. Because a range of results will be deemed acceptable, there will not be the same definite convergence of parameters as in the faulting example. The user must collect the satisfactory combinations of parameters over all generations.

In both cases above we can investigate the sensitivity of the results to changes in our chosen variables. For example, in the extension problem, a parameter such as

the saturation strain  $\varepsilon_o$  has only a weak influence on the outcome, *i.e.* it has a relatively large final range. On the other hand, parameters such as the viscosity and the pressure dependence  $B_p$  impose tight restrictions on the model behaviour. The algorithm has settled on single final values which produce the desired behaviour. With the inversion approach in general, most late-stage models are close to the target in parameter space, and so a back analysis through all generations is instructive for looking at the sensitivity of parameters.

An important component of this interactive inversion technique is its capability of suggesting surprise results. A systematic or intuitive approach relies on the experience of the modeller, and may miss realistic targets which lie outside the realm of modelling space which is envisaged. The GA, although converging upon a specific area in parameter space, also provides for random solutions. If ranked highly, such a random solution may open up an entirely different class of models which also yield realistic results.

The example inversions which we have used make use of the final static model results. However, since all forward models evolve in time, the ranking procedure may be made more sophisticated by considering the evolution of the structures involved. Multiple processes may lead to the same outcome, thus by considering the evolutionary history of the model, we may better discriminate between results. This will reduce the non-uniqueness of the inversion solution.

## **5 Conclusions**

We have demonstrated the geological application of a visual inversion algorithm. The technique of interactive evolutionary computation has considerably diminished

the effort required to explore parameter space during the inversion of conceptual models in geology. We bypass the lack of numerical data for an inversion target by using a genetic algorithm together with image ranking to focus on a visual target. This approach exploits the experience and knowledge of an expert user in a visual and therefore intuitive environment.

## References

- Boschetti, F., Dentith, M., List, R., 1996. Inversion of seismic refraction data using genetic algorithms. *Geophysics* 61(6), 1715–1727.
- Boschetti, F., Moresi, L., 2001. Interactive inversion in geosciences. *Geophysics* 66(4), 1226–1234.
- Brace, W.F., Kohlstedt, D.L., 1980. Limits on lithospheric stress imposed by laboratory experiments. *Journal of Geophysical Research* 85(11), 6248–6252.
- Goldberg, D.E., 1989. Genetic algorithms in search, optimization, and machine learning. Addison-Wesley, Reading, Massachusetts.
- Moresi, L.-N., Solomatov, V.S., 1995. Numerical investigation of 2D convection with extremely large viscosity variations. *Physics of Fluids* 7(9), 155–164.
- Takagi, H., 2001. Interactive evolutionary computation: fusion of the capacities of EC optimization and human evaluation. *Proceedings of the IEEE* (in press).
- Tarantola, A., 1987. Inverse Problem Theory. Elsevier, Amsterdam.

## Table Captions

**Table 1.** Six upper crustal parameters are free to vary during the inversion. The “best” values give rise to the top-ranked model of the last generation. The last column gives the range of parameter values for the top four models of the last generation.

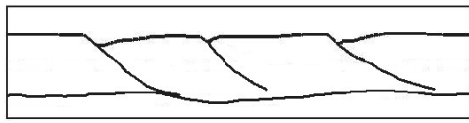
## Figure Captions

**Fig. 1.** Target image (a), initial geometry of the crust (b), and evolution of the IEC inversion. Panels (i) to (iii) represent the first two and the last generation of the GA. Images are ranked according to their similarity with the target image. Some models have not been extended to full length because of numerical non-convergence. These are left unranked, and the GA orders them randomly so as to fill up the bottom rankings.

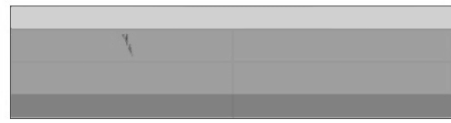
**Fig. 2.** Initial slightly perturbed layers for the folding problem (a), and final generation of the GA (b). Ranking simply includes or excludes the result from the category of multiple wavelength folding.

Table 1

Parameter	Initial range	Increment	“Best” value	Range
Viscosity	5000 - 10000	1000	9000	9000
Cohesion $B_o$	0 - 2000	200	0	0 - 200
Pressure dependence $B_p$	0 - 1.0	0.1	0.2	0.2
Tension limit $B_c$	100 - 1000	100	100	100 - 200
Maximum strain weakening $E_a$	0.1 - 0.9	0.1	0.2	0.2
“Saturation strain” $\varepsilon_o$	0.1 - 1.0	0.1	0.7	0.3 - 0.7



a



b



Rank:



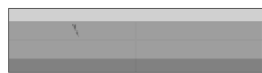
Rank:



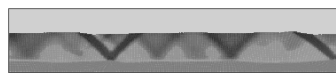
Rank:



Rank:



Rank:



Rank: 1

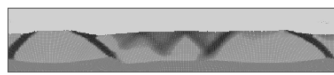


Rank:



Rank: 2

i



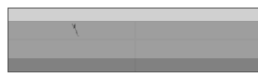
Rank: 1



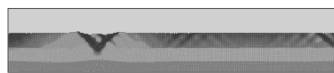
Rank: 5



Rank:



Rank:



Rank: 3



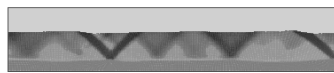
Rank:



Rank:

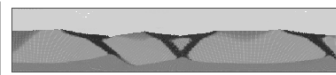


Rank: 4

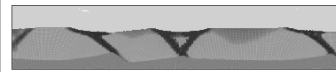


Previous best - Rank: 2

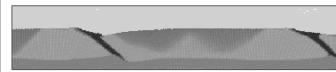
ii



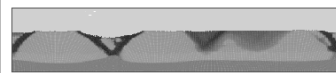
Rank: 2



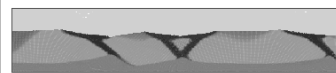
Rank: 5



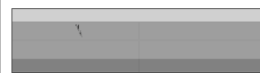
Rank: 1



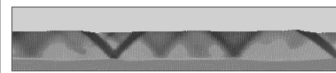
Rank: 6



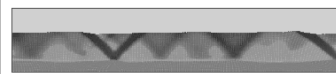
Rank: 4



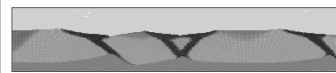
Rank: 9



Rank: 7



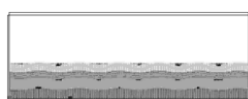
Rank: 8



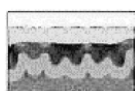
Previous best - Rank: 3

iii

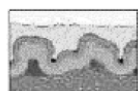
Fig. 1.



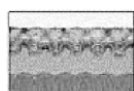
a



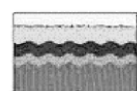
Rank: yes



Rank: yes



Rank: no



Rank: no



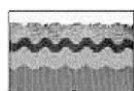
Rank: no



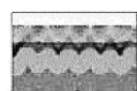
Rank: yes



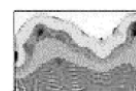
Rank: yes



Rank: no



Rank: no



Rank: yes

b

Fig. 2.